JOURNAL OF CATALYSIS **167,** 153–163 (1997)
ARTICLE NO. CA971524

# The Effect of Potassium Addition on the Surface Chemical Structure and Activity of Supported Iron

## I. FTIR Study of CO and NO Adsorption on Fe–K/$ZrO_2$

Eugenio Guglielminotti,* Flora Boccuzzi,* Francesco Pinna,† and Giorgio Strukul†

*Dipartimento di Chimica IFM, Università di Torino, Via P. Giuria 7-10125, Torino, Italy; and †Dipartimento di Chimica, Università di Venezia, Dorsoduro 2137-30123, Venezia, Italy

Received June 28, 1996; revised November 1, 1996; accepted November 6, 1996

**The surface activity of a Fe–K/$ZrO_2$ sample prepared from iron citrate and potassium carbonate has been investigated by the FTIR spectroscopy of adsorbed CO and NO and compared with the behavior of a Fe/$ZrO_2$ sample. The addition of potassium produces a strong decrease of the BET area and of the amounts of the adsorbed molecules. At the same time the spectrum of the sample reduced with $H_2$ at 573–773 K shows, under anhydrous conditions, the presence of small patches of reduced $Fe^0$, not easily formed on Fe/$ZrO_2$ under the same thermal and reducing conditions. The formation of new phases containing iron and potassium in close combination, such as mixed iron–potassium oxalates and potassium ferrites that fully cover the zirconia surface, was inferred from FTIR data. CO adsorption favors the partial surface reduction of these phases producing small Fe-carbonyl clusters in tight contact with potassium and Fe,K-carboxylate surface species. The adsorption of NO, producing nitrosyl species on the reduced iron particles and nitrite groups on the potassium phase is in good agreement with the results of adsorbed CO. These results are confirmed by quantitative determinations of adsorbed gases and by TPR experiments.** 

### INTRODUCTION

The structural effects of potassium or other alkali metals on the chemical composition and the catalytic activity of systems based on supported or unsupported iron have been extensively studied and discussed since the beginning of this century, particularly because of the importance of these catalytic systems in the synthesis of ammonia.

It is now established (1) that the addition of evaporated metallic potassium to monocrystalline iron (2) or to other transition metals produces an electron transfer to the metal. As a consequence of the increased electron density, the metal is available for the back-bonding to the $2p^*$ orbitals of CO and diatomic adsorbed molecules, enhancing their dissociation capacity. Therefore, the effect of K promotion is to improve the activity of iron based catalysts, as is widely known for example in the Fischer Tropsch (FT) and ammonia synthesis, reactions in which CO and $N_2$ dissociation are needed. However, these electronic effects have been experimentally confirmed only by addition of metallic, nonionic potassium on unsupported iron (or other transition metals) kept in the zerovalent state under ultrahigh vaccum (UHV) conditions.

However, the experimental conditions under which the iron based catalysts are used for the FT or ethylbenzene to styrene reactions are quite different. These catalysts consist of oxidized iron phases with addition of ionic potassium promoters, such as $K_2O$ or $K_2CO_3$, and are active under conditions that are only mildly reducing because of the presence of steam which can oxidize both the iron and the potassium components. Moreover, the formation of new phases such as ferrites ($KFeO_2$ and similar) has been clearly established (3–5). Since in this case, at least in the bulk of the new phase, both iron and potassium are oxidized, the effects of electron transfer should be null or strongly reduced and the zerovalent iron formed with difficulty.

As to the catalyst of ethylbenzene dehydrogenation, its active state was demonstrated to be a metastable mixture of magnetite and potassium ferrite phases (3, 4). In this case the electron-donation effect of potassium to $Fe^0$ crystals might be excluded, although the oxidation state of the active centers on the iron surface should be affected by potassium addition and difficult to determine (6).

A metastable equilibrium $Fe^{3+}/Fe^{2+}$ controls the valence states of iron oxides in massive phases (7), but the formation on the surface of highly dispersed zerovalent iron phases cannot be excluded in reducing conditions and under vacuum. This hypothesis is most likely valid for supported iron systems in the presence of potassium promoters. In these systems iron may interact both with the support, forming mixed iron–support phases (iron silicates, aluminates, titanates, etc.), and with the potassium forming $KFeO_2$ and related polyferrite phases. Besides, the addition of K-based



0021-9517/97 $25.00

promoters such as KOH and $K_2CO_3$ causes a long resistance to deactivation suppressing coking (1). Coke deposition with possible formation of iron carbide or oxicarbide phases (8) and the simultaneous reduction of $\alpha$-$Fe_2O_3$ to magnetite and/or ilmenite-like FeO and $Fe^0$ phases (5, 7, 9) in strongly reducing conditions greatly complicates the picture of the phases involved in the numerous, very important, hydrogenation–dehydrogenation reaction steps in which K-promoted iron systems are active.

In this paper we wish to contribute to the knowledge in this field, with the warning that the conclusions are strictly valid only for the experimental system studied, but, at the same time, we hope to enlighten the more general debate on the promotion effect of potassium. In previous papers (10, 11) one of us studied zirconia supported iron ($Fe/ZrO_2$) with 1% wt Fe in order to evidence the surface interactions of iron dispersed on the support. In this system a metastable solid solution of ferrous ions on the zirconia surface is formed at 623 K in hydrogen and this is reduced with difficulty to $Fe^0$ even at 773 K. The FTIR spectra of adsorbed CO and NO were utilized to show the high iron dispersion and heterogeneity of sites with respect to both the coordination and the oxidation numbers.

On the same $Fe/ZrO_2$ system the addition of small amount of potassium as $K_2CO_3$ results in an easier reduction to zerovalent iron dispersed on the surface as is evidenced by FTIR experiments of CO and NO adsorption. Therefore, the results here reported show that the addition of potassium, even as ionic compound, favors in anhydrous conditions the reduction of highly dispersed iron to zerovalent Fe microcrystals. The comparison between the $Fe/ZrO_2$ and $Fe–K/ZrO_2$ spectroscopic data gives an experimental unequivocal evidence of the effect of K addition on the surface state of supported iron catalyst.

## METHODS

The sample was prepared by coimpregnation of solutions of ferric ammonium citrate and potassium carbonate on $ZrO_2$ (BET = 10.4 $m^2/g$) prepared by hydrolysis of $ZrOCl_2$ with $NH_4OH$ and calcined at 1100 K for 8 h. After Fe,K impregnation the sample was dried at 383 K and then calcined at 973 K for 2 h. During $ZrO_2$ preparation by hydrolysis, $Cl^-$ was clearly present on the $Zr(OH)_4$ precipitate. However, it is our standard procedure to wash the precipitate thoroughly with distillated water until negative $AgNO_3$ test: after this procedure, residual $Cl^-$ on $ZrO_2$ calcined at 823 K, determined by X-ray fluorescence, was found to be around 0.05%. Neutralization of residual $Cl^-$ by KOH will probably take place. The metal loading, determined by A A spectroscopy, was 2 wt% Fe and 1.06 wt% K, yielding a molar ratio Fe/K of 1.4 (hereafter FK1). The BET surface area of the calcined sample decreased slightly to 9.7 $m^2/g$. but it increased again to 11.9 and 11.7 $m^2/g$ after reduction at 623 and 773 K, respectively. These values should be compared with the value of 61 $m^2/g$ obtained for $Fe/ZrO_2$ reduced at 623 K prepared by impregnation of an high area support (10). Other samples were prepared in the same way but starting from ferric nitrate and calcined for 2 h at 773 K, containing 2.02% Fe-1.21% K (FK2) or 1.96% Fe–0.66% K (FK3).

Quantitative adsorption experiments with CO and NO at room temperature on FK1 gave values of $2.7 \times 10^{-3}$ and $4.0 \times 10^{-2}$ mol/mol Fe, respectively. The corresponding values found on $Fe/ZrO_2$ were 0.115 and 0.48 (10). The BET and the quantitative results are reported in Table 1.

FTIR spectra were recorded at RT on a Perkin Elmer 1760 instrument, equipped with a MCT cryodetector, with 2 $cm^{-1}$ resolution and with 64–128 scans accumulation and with substraction of the background after the indicated thermo-chemical treatments. The FTIR results of CO and NO adsorption are obtained with a pellet of the sample outgassed and reduced *in situ* for 15 min under 100 mbar $H_2$ at 573, 673, and 773 K (hereafter FK1(573), etc.), with a final outgassing at the same temperatures to eliminate water and carbon dioxide formed during the reduction. Survey experiments here not reported show that the outgassing at the same temperatures without reduction yielded samples that were not very different in surface activity with respect to the reduced ones.

FTIR experiments, not reported here in detail, with FK2 and FK3 samples were performed for comparison among samples prepared under different thermal and chemical conditions.

Temperature programmed reduction measurements (TPR) were performed in a previously described standard apparatus (13). The samples were calcined *in situ* at 773 K (1 h) with a 5% $O_2$ in Ar mixture, cooled down to room temperature, and then heated at a linear rate of 10 K/min from 298 to 1073 K with a gas (5% $H_2$ in Ar) mixture (40 ml/min). Quantitative measurements of hydrogen consumption were performed by calibrating the system with a known amount of hydrogen.

**TABLE 1**

**Quantitative Data on Fe, $FeK/ZrO_2$ Systems**

| System | Area BET ($m^2/g$) | CO, 298 K (mol/mol Fe) | NO, 298 K (mol/mol Fe) | TPR $H_2$/Fe consumption |
|---|---|---|---|---|
| FK1 | | | | |
| Oxidised 973 K | 9.7 | — | — | 2.1 |
| Reduced 623 K | 11.9 | — | — | |
| Reduced 773 K | 11.7 | $2.7 \cdot 10^{-3}$ | $4.0 \cdot 10^{-2}$ | |
| FK3(773) | | | | 0.61, 0.74 |
| $Fe(1\%)/ZrO_2(623)$[a] | 61 | 0.115 | 0.48 | 0.93 |

[a] Ref. 10.

CO and NO chemisorption measurements were performed using a pulse flow technique (13). Prior to measurement, the sample was subjected to a thermal pretreatment which involved: (i) exposure to Ar at 773 K for 30 min, (ii) an injection of 10 pulses (3 ml each) of a reductive gas (5% $H_2$ in Ar) mixture, and (iii) He purge at the same temperature for 15 min. The sample was then cooled in He flow to 298 K for CO and NO chemisorption experiments.

The Fe and K contents were determined by atomic absorption spectroscopy.

Gas of ultrahigh purity from UCAR were utilized without further purification, except for NO which was freshly distilled by cryo-condensation cycles.

## RESULTS

### *FTIR Spectra of Adsorbed CO*

As a preliminary observation, the spectra of FK1(773) show, as reported in the literature (12), that K addition to Fe/$ZrO_2$ nearly completely eliminates the hydroxyl surface groups, leaving only very weak bands at 3680 and 3434 $cm^{-1}$, tentatively assigned to free OH groups on iron (14) and potassium oxides (15), respectively.

Figure 1 shows the FTIR spectrum of CO adsorbed at RT on the FK1(573) sample at increasing contact times. The frequency range and the increasing intensity of the bands of adsorbed CO shows that at RT an activated process of CO adsorption, produces carbonyls in different configuration plus carbonate–carboxylate groups (see the band at 1660 $cm^{-1}$). The spectrum is limited to 1650 $cm^{-1}$ because, at lower frequencies, no intense bands are clearly distinguished because of the very low transparency of the sample, which contains strong residual carbonate-like bands in the

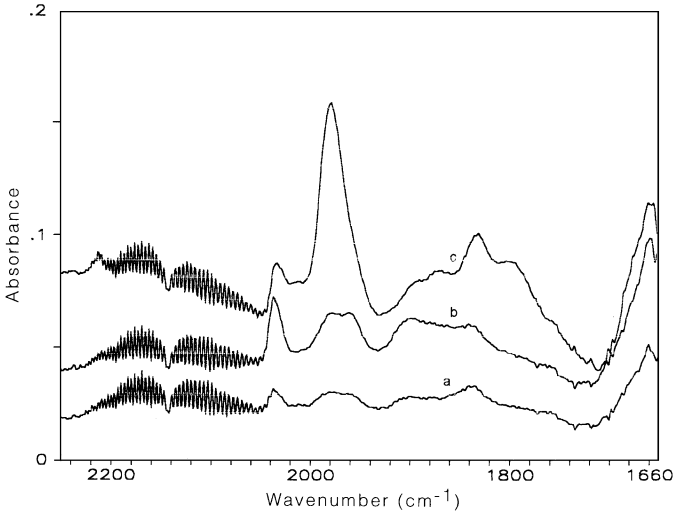


**FIG. 1.** FTIR spectra of CO adsorbed at RT on FK1(573). Curve a, immediately after contact with 43.5 mbar CO; curve b, after 20 min; curve c, after 16 h.

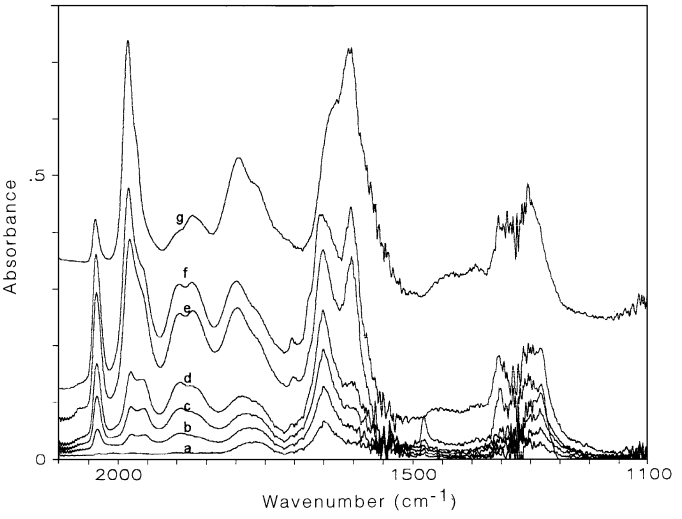


**FIG. 2.** FTIR spectra of CO adsorbed on FK1(673). Curve a, after contact with 1.5 mbar CO; curve b, after contact with 19.6 mbar CO, immediately; curves c–e, spectrum recorded after15 min, 30 min, and 16 h, respectively; curve f, after outgassing for 5 min at 300 K; curve g, after outgassing for 15 min at 423 K.

background. However after 16 h the maximum absorbance of the bands is ~0.1. Only the rotational contour of the stretching mode at 2143 $cm^{-1}$ of CO gas in the cell with a small optical path is evident at $\nu \geq 2050$ $cm^{-1}$. In this spectral region no bands assignable to CO species reversibly chemisorbed on ionic zirconium or iron sites (10) appear, as was previously observed on the Fe/$ZrO_2$ sample. The weak bands approximately centered at 2036, 1980–1960, 1900–1830–1797, 1660 $cm^{-1}$ change strongly in relative intensity and slightly in frequency.

Figure 2 shows the spectrum of CO adsorbed on the same sample FK1(673) in the range 2100–1100 $cm^{-1}$: the slight increase of transparency in the low frequency region of the background due to the higher temperature of outgassing allows the spectrum to be shown also in the 1650–1100 $cm^{-1}$ range. The cutoff of the background at 1100–1000 $cm^{-1}$, due to the lattice modes of the support, produces spectra with an intense noise, but no bands are found in and below this range and the same holds for the FK1(773) sample.

The general features the spectrum of CO adsorbed on the sample reduced at 673 K (Fig. 2) are not very different from those of the sample reduced at 573 K, as far as the frequencies of the surface species and their behavior with the contact time are concerned. However, the intensity of the carbonylic bands at 2037, 1981, 1956sh, 1895, 1870, 1793, 1762sh $cm^{-1}$ (curves a–f) is about three times larger with respect to that reported in Fig. 1. The same increase in intensity with the contact time is observed for the bands at 1650, 1601, 1354, 1300–1282 $cm^{-1}$. During the slow process of CO adsorption the overall transmittance of the sample decreases, indicating that a reductive reaction induced by

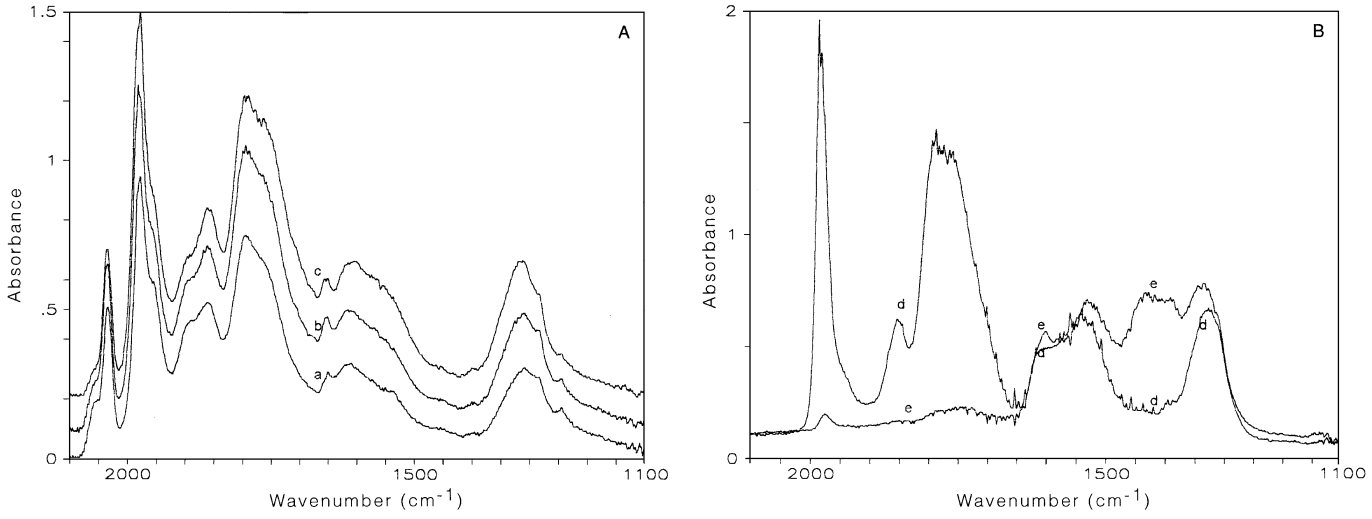


**FIG. 3.** FTIR spectra of CO adsorbed on FK1(773). (A) Curve a, after contact with 57.7 mbar CO; curve b, spectrum after 15 min; curve c, after outgassing for 5 min at 300 K. (B) Curves d and e, after outgassing for 15 min at 423 and 523 K, respectively.

CO adsorption occurs at the surface. The same effect is found for CO adsorption on the sample reduced at 773 K (see Fig. 3).

The outgassing of CO at 423 K (curve g) produces the decrease of the bands at 2037, 1956, 1895, and 1650 cm$^{-1}$, whereas the bands at 1981, 1870, 1793–1762, 1601, and ~1300 cm$^{-1}$ have constant or slightly increased intensity: this behavior shows an equilibrium and an interconversion of adsorbed species which depends on the temperature and on the CO pressure. After outgassing for 30 min at 523 K all the iron-carbonylic bands in the range 2050–1700 cm$^{-1}$ are removed from the spectrum and CO readsorption restores the same spectrum: this seems to show a rather stable surface arrangement.

Figure 3 shows that the results of CO adsorbed on FK1(773) sample are qualitatively not different from those reported in Figs. 1 and 2, but the overall intensity of the bands increases further (about 4 times with respect to FK1(673) and 12 times with respect to FK1(573)). Only the broad bands at 1794–1762 cm$^{-1}$ increase in their relative intensity. Also for this sample the CO adsorption is an activated process at RT (main peaks at 2058sh, 2036, 1982, 1956sh, 1894sh, 1862, 1794–1762, 1650–1600, and 1310–1282sh cm$^{-1}$); i.e., the species formed at the surface strongly increase in their total concentration with the increase of the temperature of reduction, but they change only slightly in their structure and relative concentration.

In agreement with the results of Fig. 2, Fig. 3 (curves c, d) shows that the carbonyl species correlated to the bands at 1982, 1862, and 1794–1762 are resistant to outgassing and they are weakly increasing in intensity, whereas those correlated to the bands at 2058, 2036, 1956, and 1895 cm$^{-1}$ disappear or are converted to the more resistant ones by a process of surface fluxionality.

A frequency shift and a conversion of the species are also noticed in the low frequency region for the bands at 1650, 1600, and ~1300 cm$^{-1}$ and for the bands now centered at 1536 and 1324 cm$^{-1}$. Outgassing at 523 K (curve e) produces the nearly complete elimination of the intense bands at 1982, 1862, and 1794–1762 cm$^{-1}$. At the same temperature strong changes are noticed for the bands at low frequency with shifts to 1530 and 1334 cm$^{-1}$ and the growth of new broad bands at 1430–1338 cm$^{-1}$. CO readsorption at RT on the 523 K outgassed sample (data not reported for the sake of brevity) restores nearly completely (the intensity is reduced of only one-third) the spectrum reported in Fig. 3A, curve a, showing that the process of CO adsorption occurs mainly at the surface and is almost completely reversible.

The growth of the bands in the carbonate-like spectral region accompanied by the decrease of Fe-carbonylic bands between 2050 and 1700 cm$^{-1}$ by outgassing at 423–523 K is an interesting occurrence that deserves further attention.

Figure 4, curve a, shows the difference between the spectrum after CO evacuation at 523 K and that of CO adsorbed and evacuated at RT; curve b shows the same difference, but of a different experiment with the gas phase heated in a closed cell, without desorbate elimination at 523 K; both experiments were performed on the same FK1(773) sample. For the two different treatments the Fe-carbonylic bands are fully eliminated and appear as negative peaks, but the positive broad peaks with maxima at 1603, 1530, 1416, and 1345 cm$^{-1}$ are more intense in curve b, i.e., if carbon monoxide or dioxide are not desorbed. The previous desorption experiments show the reversibility of adsorbed CO; however, it is hypothesized that the growth of carbonate groups leads to the transfer of CO onto the oxygens of the oxidized potassium or iron phases and, in presence of gas phase, the

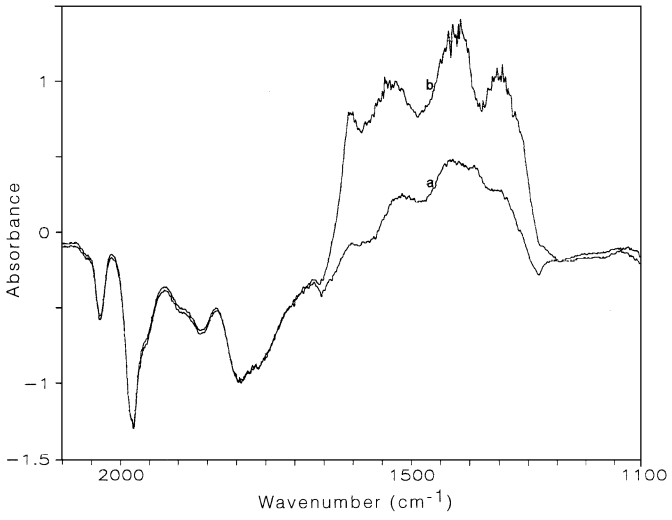


**FIG. 4.** Difference spectra of CO heated or outgassed at 523 K and adsorbed at 300 K. Curve a, spectrum of the sample saturated with 41.1 mbar CO and outgassed for 15 min at 523 K minus that of the sample saturated with CO at 300 K ; curve b, the same as curve a, but with the sample heated for 15 min at 523 K in CO atmosphere.

conversion from carbonyl to carbonate-like groups with an iron induced CO disproportionation.

In Fig. 5 the difference between the background spectrum of FK1(573) and those of FK1(673) and FK1(773) samples is reported in the range 1800–1000 $cm^{-1}$; the two strong and broad absorptions at 1620sh–1580 and 1320sh–1308 $cm^{-1}$ are clearly correlated to surface species desorbed

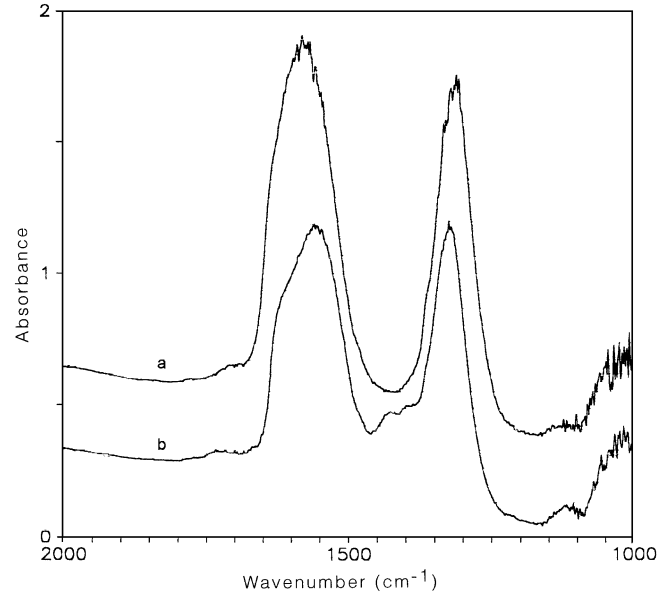


**FIG. 5.** Difference between the backgrounds of FK1 obtained at 573, 673, and 773 K. Curve a, difference between FK1(573) and FK1(773) backgrounds; curve b, difference between FK1(673) and FK1(773) backgrounds.

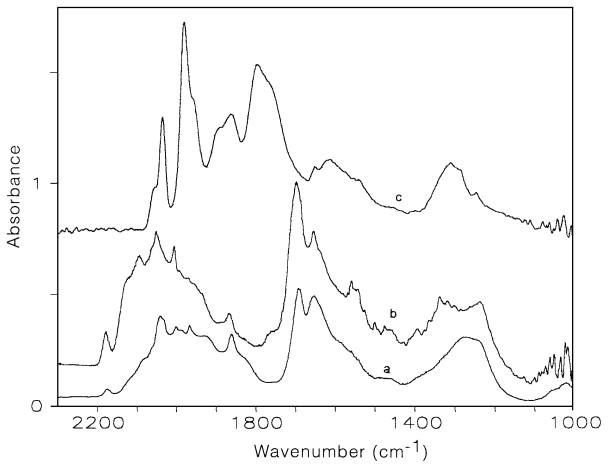


**FIG. 6.** FTIR spectra of CO adsorbed at RT and saturation on FK1, FK2, and FK3(773) samples. Curve a, FK3 sample contacted with 29.4 mbar CO; curve b, FK2 sample contacted with 21.2 mbar CO; curve c, FK1 sample contacted with 41.1 mbar CO.

in the temperature gradient 573–773 K. No bands are clearly evident in the 1100–1000 $cm^{-1}$ range.

In Fig. 6 the spectra of CO adsorbed at saturation on differently prepared Fe–K/$ZrO_2$ samples reduced at 773 K are reported for comparison. Curve c refers to the FK1 samples, curves b and a refer to the FK3 and FK2 samples prepared from iron nitrate with 0.66 and 1.21% K, respectively. We have studied the CO adsorption on these samples in detail, but the data are here summarized for the sake of brevity. The main differences between the FK1 and the ex-nitrate samples are:

(i) The higher intensity of the Fe-carbonylic bands at 2050–1700 $cm^{-1}$, with new peaks at 2044, 2004, 1968, and 1918 $cm^{-1}$ and the lower intensity of the bands at 1700–1000 $cm^{-1}$ of the FK1 sample. New intense bands are formed at 1695–1650 and 1340–1250 $cm^{-1}$ and the FK2 sample shows weak bands at 1055–1020 $cm^{-1}$.

(ii) The nearly complete absence of the strong broad absorption at 1794–1762 $cm^{-1}$ and the reduced intensity of the 2036, 1982, and 1895–1860 $cm^{-1}$ bands on the FK3 and FK2 samples. However, on these samples the discrete peaks are very numerous in the range 2100–1800 $cm^{-1}$ or seem to be superimposed to a broad band at ~2000 $cm^{-1}$ assigned to CO adsorbed on large $Fe^0$ particles (16–19).

(iii) The presence on FK3 and FK2 of bands at 2180 and 2115–2080 $cm^{-1}$ assigned to CO adsorbed on coordinatively unsaturated $Zr^{4+}$ or $Fe^{2+}$ ions, respectively, although with minor intensity with respect the Fe/$ZrO_2$ system. The experiments not reported here show that these species are reversible at RT, similarly to the Fe/$ZrO_2$ system (10).

However, the calcination of FK2 and FK3 at 973 K produces samples which show the same surface activity toward CO, i.e., lack of bands at 2180–2080 $cm^{-1}$ and formation of the same carbonyl groups shown in Figs. 1–3.

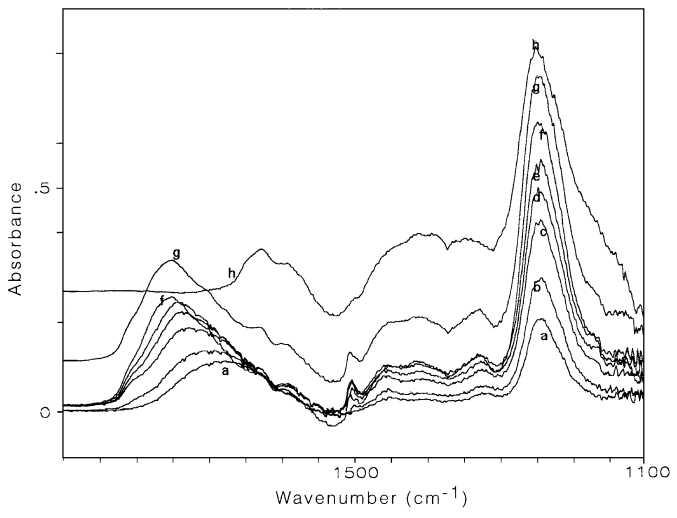


**FIG. 7.** FTIR spectra of NO adsorbed on FK1(773) sample. Curves a–d, after contact with 0.1, 0.4, 1.6, and 3.3 mbar NO, respectively; curves e, f, as f, after 15 min and 3 h, respectively; curve g, after outgassing for 5 min at RT; curve h, after outgassing for 15 min at 423 K.

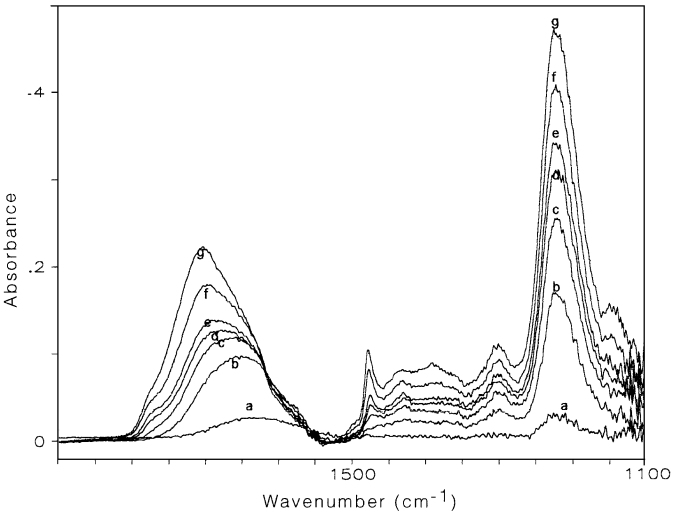


**FIG. 8.** FTIR spectra of $^{15}NO$ adsorbed at RT on FK1(773) sample; curves a–g, after contact with 0.1, 0.4, 0.6, 0.8, 1.1, 3.0, and 5.5 mbar $^{15}NO$, respectively.

### *FTIR Spectra of Adsorbed NO*

Figure 7 shows the FTIR spectra of NO adsorbed on the FK1(773) sample at increasing pressures and contact times. The increase in intensity of a broad band in the nitrosyl stretching region, and the shift with the coverage from 1675 to 1752 $cm^{-1}$ with a shoulder at 1803 $cm^{-1}$ at higher coverages is accompanied by the growth of a strong band at constant frequency 1245 $cm^{-1}$ and by weak bands at 1327, 1410, 1456, and 1506 $cm^{-1}$, a process that is exactly parallel to that shown by CO. A very weak combination band (not shown in the figure) at 2564 $cm^{-1}$ grows with an identical behavior. The outgassing at 423 K results (curve h) in the complete elimination of the nitrosylic weak band. Weak components of difficult assignment remain at 1620–1590 $cm^{-1}$, whereas the bands at 1327 and 1245 $cm^{-1}$ slightly decrease.

The experiment of $^{15}NO$ (99%) adsorption on the same FK1 sample, reported in Fig. 8, produces a spectrum almost identical to that of Fig. 7, with all the bands red-shifted by the expected 0.982 theoretical ratio. The fitting is quite good for the nitrosylic absorption, with some difficulty in reproducing exactly an identical coverage and time of contact and in identifying the intensity maximum of very broad bands, while it is excellent for the other bands. Figures 7 and 8 give a good picture of the close resemblance of the NO and $^{15}NO$ adsorption results obtained on the FK1 sample.

### *TPR and Chemisorption Experiments*

The TPR of $Fe/ZrO_2$ ex-nitrate (Fig. 9, curve a) shows only one reduction peak at 573 K which may be assigned to the partial reduction of $Fe_2O_3$ on the basis of its intensity. A quantitative estimate of the amount of hydrogen consumed indicate a $H_2/Fe$ ratio of 0.93, i.e., lower than the theoretical value of 1.5 expected for complete reduction to $Fe^0$. This peak is present also on the samples containing potassium (Fig. 9, curve b) even if shifted to 623 K. However, in this case a second peak appears at 773 K and the quantitative analysis of the two peaks indicates $H_2/Fe$ ratios of 0.61 and 0.74, respectively. The very broad peak at ~1000 K can be assigned to the reduction of the $K_2CO_3$ phase, in agreement with its growth with the increase of the potassium amount and with the analogous assignment of Stobbe (5).

A more complex behavior is shown by the samples prepared from citrate with potassium (Fig. 9, curve c). Here the main peak of reduction is present at 765 K and can be related to a direct reduction in one step of $Fe^{3+}$ to $Fe^0$. However, in this case the quantitative analysis indicates a

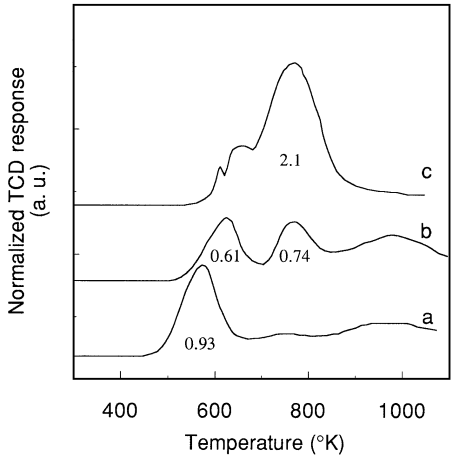


**FIG. 9.** TPR profiles, normalized to the iron percentage, of catalysts made from nitrate (a, $Fe/ZrO_2$; b, FK3) and citrate (c, FK1). Numbers below the individual peaks indicate the $H_2$ consumption expressed as $H_2/Fe$ mole ratio.

$H_2$/Fe ratio of 2.1 well above the theoretical value. In addition, two small peaks at 610 and 650 K could be related to a minor process of reduction to $Fe^0$ occurring at the surface of iron, i.e., at temperatures lower than 773 K because of the close contact between iron and potassium. In this case the broad TPR peak of $K_2CO_3$ reduction at 1000 K is not observed, but the TPR results support the full reduction of a $KFeO_2$ phase.

## DISCUSSION

As a preliminary consideration we recall that unambiguous structural data on the FK1 system could not be obtained by X ray technique because of the lack of unequivocal instrumental signals other than those of zirconia due, *inter alia*, to the low percentage of iron and potassium. Similarly undetected was the formation of the not well defined and amorphous $KFeO_2$ phase, as in the case of metastable Fe/$ZrO_2$ solid solution (10), because, in agreement with the literature (3–5, 12), this can be detected by X ray diffraction only on samples containing 10% Fe and increasing amounts of K, due to its instability when exposed to the air atmosphere.

The BET analysis shows that the area of samples containing iron and potassium in low quantity decrease only slightly after calcination and increase only slightly after reduction with respect to the area of the sample without iron. Moreover, a comparison of the quantitative CO and NO adsorption results shows that the potassium addition to the Fe/$ZrO_2$ systems reduced under the same conditions, decreases more than one order of magnitude the total amount of these gases adsorbed on iron and more than five times with respect to the sample containing only iron. From these results a strong change of the number and of the environment of surface iron atoms by potassium addition, favored by the formation of a new phase containing iron and potassium in a close contact, may be inferred.

Therefore the FTIR results on CO and NO adsorption and their comparison with the previously published results on the Fe/$ZrO_2$ system (10, 11) are the main source of information on the nature of the surface sites exposed to the adsorbate. Some hypotheses on the surface structure of the catalyst can be extrapolated from this information. For example it can be said, at least for the FK1 sample, that the surface of zirconia is fully covered by a phase (or phases) containing iron and potassium; in fact, CO adsorption does not reveal the presence of any exposed $Zr^{4+}$ sites as found either on pure zirconia (20) or, even in lower concentration, on Fe/$ZrO_2$ (10). In fact, Fig. 6 shows that the band at 2180–2190 assigned to CO weakly chemisorbed on $Zr^{4+}$ sites is absent on the FK1 sample and very weak on the FK2 and FK3 samples and decreases with increasing K percentage. The surface coating of a phase containing iron and potassium is probably responsible of the nearly constant values of the areas ($\approx$10 $m^2$/g) observed on differently treated FK1 samples and on $ZrO_2$.

A similar behavior is observed in NO adsorption: the nitrosylic bands are strongly lowered in intensity and changed in frequency by K deposition as in the Fe/$Al_2O_3$ system (21) and the band at 1180 $cm^{-1}$, previously assigned to the $NO_2^-$ group formed on the zirconia surface (11), is absent and substituted by a band at 1245 $cm^{-1}$ assigned to a potassium nitrite group (22) (see Fig. 7 and the relevant discussion).

To discuss the spectra reported in Figs. 1–3 of CO adsorbed on the FK1 sample reduced and outgassed at increasing temperatures, it seems useful to summarize their main features.

The adsorption of CO is an activated process at RT, which produces increasing quantities of adsorbed species both in the carbonyl (2050–1700 $cm^{-1}$) and in the carbonate–carboxylate (1700–1000 $cm^{-1}$) regions of the spectrum. Therefore, CO is adsorbed on reduced metallic sites and the former IR bands are attributed to CO adsorbed in the linear and/or bridged form to $Fe^0$. These sites may be either already existent on the surface after the reducing–outgassing treatment or may be formed by a slow CO reduction process. The latter IR bands are attributed to carbonate–carboxylate species formed by CO adsorbed on already existent oxidized Fe–K surface sites and/or formed by a redox process on the surface by CO itself. The latter hypothesis is confirmed by the noticeable decrease in transparency of the sample after contact with CO at RT, which can be explained only by the slow reduction process of a *n*-semiconducting ferric phase.

The experiments of CO desorption at 423 K (see Fig. 2, curve g, and Fig. 3B, curve d) allow differentiation between carbonylic species that are resistant at this temperature (bands at 1982, $\sim$1862, and 1794–1762 $cm^{-1}$) and other more weakly adsorbed carbonylic species (2058–2036, 1956, 1895 $cm^{-1}$). The literature IR data of CO adsorbed on $Fe^0$ particles, either supported and evaporated as microcrystals (16), or on monocrystals exposing well defined Fe surfaces as (111) (17, 18) or (100) (19) are in agreement with the assignment of the carbonylic bands at $\nu \geq 2000$ $cm^{-1}$ to CO adsorbed linearly on top of the $Fe^0$ first layer sites (the bands at 1982–1956 $cm^{-1}$ may be attributed to slightly tilted linear species). The bands at 1900–1800 $cm^{-1}$ are assigned to bridged CO adsorbed on the second layer shallow hollow sites, following the notation of Ertl and co-workers (17) for Fe(111). The bands in the range 1800–1700 $cm^{-1}$ are of more difficult assignment, but they are increased in intensity by increasing the potassium composition (2, 18, 19) and therefore they may be assigned to either $Fe^0$ $\mu$-bridged CO or to linear or bridged CO species adsorbed on $Fe^0$ sites perturbed by neighbouring potassium atoms. The large number of the peaks in the range 2050–1700 $cm^{-1}$ can be rationalized on the basis of small $Fe^0$ crystallites showing a large heterogeneity of the exposed sites.

However, if this model could be extended to all the iron phase, it should produce a large Fe dispersion and a consequent large amount of adsorbed CO. This was in conflict with the quantitative CO adsorption results that show a very small total coverage by CO (less than 1% in Fe moles). The residual iron phase is coated by potassium. Therefore the FTIR data cannot be discussed in terms of CO adsorbed on large sized exposed faces, but rather in terms of CO adsorbed on a few and small iron clusters formed by reduction at the interface of Fe–K phases. Indeed, organometallic carbonyl clusters show carbonylic bands with very high extinction coefficients (23). The spectra shown in Figs. 1–3 in the range 2050–1700 $cm^{-1}$ seem therefore in agreement with the formation of iron–carbonyl clusters in low concentration. This hypothesis is also in agreement with their constant frequency, independent of the coverage, and the narrow halfwidth of the bands (in particular of those at 2036 and 1982 $cm^{-1}$). We can therefore conclude that only a few, small $Fe_nCO_m$ clusters (with $n$ and $m$ very small) are formed at the surface of a phase containing both iron and potassium (for the bands at 1794–1760 $cm^{-1}$, see Table 2). The desorption experiments show that at least two types of clusters with different $n$ and $m$ values and with different thermal stability are formed. The region of their CO stretching bands is consistent with zerovalent iron clusters, but also with the adsorption spectra of some carbonylferrates (Table 2) formed by reduction of iron carbonyls of small nuclearity with alkali hydroxides according to the general scheme (23)

$$Fe_n(CO)_m + 4OH^- \rightarrow [Fe_n(CO)_{m-1}]^{2-} + CO_3^{2-} + 2H_2O \quad (n = 1\text{–}4,\ m = 5, 9, 12, 14).$$

This scheme, that is convincing in solution, should be modified for reactions on a surface outgassed at 773 K, in which the hydroxyls are very few, although it contains some suggestions that can be considered valid also for our samples in which basic hydroxyl groups can be easily formed both by reduction of oxides with hydrogen and by hydrolysis of $K_2CO_3$. Indeed, the spectra of Figs. 1–3 show the simultaneous formation of broad bands at 1660–1600 and 1310–1280 $cm^{-1}$, i.e., in a region compatible with the stretching modes of surface bidentate carbonates (24), although the loss of the $\nu_1$ carbonate mode at ~1050 $cm^{-1}$ is to some extent not consistent with this assignment and the band at 1450 $cm^{-1}$ of bulk $K_2CO_3$ (25) is not formed. The broad bands shown in our spectra are in full agreement with the spectrum of oxalate compounds such as $K_2C_2O_4$ absorbing at 1650–1600 and 1320–1308 $cm^{-1}$ (26) or $FeC_2O_4 \cdot 2H_2O$ absorbing at 1640 and 1320 $cm^{-1}$ (27). These compounds

**TABLE 2**

**IR Bands and Assignments of Fe, FeK, and Fe Carbonyl Systems**

| System | Frequencies ($cm^{-1}$) | Assignment | References |
|---|---|---|---|
| Fe evaporated in UHV | 2040–1915 | Linear CO stretching | 16 |
| Fe supported on oxides | 2035–1925 | Linear CO stretching | 16 |
| Fe(111) | 2000 | CO on top | 17 |
| | 1850–1800 | CO on shallow hollow | |
| | 1530 | CO on deep hollow | |
| Fe(100) | 2015–1940 | CO on top | 18 |
| | 1860–1760 | CO on shallow hollow | |
| Fe(111) + K | 2000 → 1740 (Shifts $\theta_K$) | CO on top | 2 |
| | 1850 → 1820 (Shifts $\theta_K$) | CO on shallow hollow | |
| | 1530 → 1580 (Shifts $\theta_K$) | CO on deep hollow | |
| | 1360 → 1435 (Shifts $\theta_K$) | CO on K modified sites | |
| Fe(100) + K | 1750(Fe/K = 2) | CO on top | 19 |
| | 1550 | $K_x(CO)_y$ species | |
| $Fe(CO)_5$ | 2034, 2013 | Linear CO stretchings | 23 |
| $Fe_3(CO)_{12}$ | 2043, 2020, 2008–1997 | Linear CO stretchings | 23 |
| | 1865, 1834 | Bridged CO stretchings | |
| $[Fe_3(CO)_{11}]^{2-}$ | 1941, 1913, 1884 | $\nu$CO | 23 |
| $[Fe_4(CO)_{13}]^{2-}$ | 2030, 1967, 1950, 1829 | $\nu$CO | 23 |
| $Fe/ZrO_2$(773) | 2192–2184 | $Zr^{4+}$–CO | |
| | 2140–2100 | $Fe^{2\pm x}$–CO | 10 |
| | 2066, 2045, 2024, 2018 | $Fe_x(CO)_y (x \approx 3)$ | |
| | 1990–1970 | $Fe^0$–CO | |
| FK1(773) | 2058, 2036, 1956, 1895 | $\nu$CO of $Fe_n(CO)_m$, 423 K depleted | This work, see Discussion |
| | 1982, 1862, 1794–1762 | $\nu$CO of $Fe_xK_y(CO)_z$, 473 K depleted | |
| | 1650–1600 | $\nu_a$OCO of KFe-oxalates | |

can be easily formed already during the preparation of the catalyst for the reducing action of citrate and ammonium anions on the potassium carbonate, with formation of an intermediate mixed $K_2Fe(C_2O_4)_2$ species as reported in the literature (28). Under reducing conditions at 573–773 K small amounts of metallic iron may catalyse the reduction of $K_2CO_3$ (normally stable until 1100 K) as suggested by the reduction of this compound at 570 K when deposited on Fe-foil (6, 29, 30). Then the oxalates formed may be decomposed with the possible formation of the $KFeO_2$ phase (and $Fe^0$) as indicated in the literature (3–5, 12). The divalent iron, stabilized by the support alone (10), when in contact with potassium can be at the same time oxidized to $Fe^{3+}$ and reduced to $Fe^0$. The latter, in CO atmosphere, forms iron clusters of zero (or lower, if carbonylferrates are formed) valence state. At the same time, the oxalate groups are either thermally decomposed at 573–773 K to formate and then to CO and $CO_2$ species, or remain undissociated as residual potassium oxalates. Figure 5 shows that the species evacuated from 573 to 773 K are related to oxalate rather than to carbonate groups because the $\nu$(sym) C–O mode at $\sim$1050 $cm^{-1}$ is not found. In CO atmosphere, for the rule of microscopic reversibility, the decomposed oxalate groups can be slowly reformed together with the reduced Fe carbonyl clusters; the redox activity of CO is evident from this scheme, showing also that CO is not an innocent spectator on the surface.

The general picture of the FK1 sample is therefore that of a zirconia surface covered with a phase containing both iron and potassium (for example as $K_2Fe(C_2O_4)_2$, $KFeO_2$, or similar "sheet structure" compounds (31)) which fully poisons the acid $Zr^{4+}$ sites and the surface hydroxyls. This hypothesis is in agreement with the elimination of residual hydroxyls on the zirconia surface and the null pyridine adsorption reported in literature (12). These phases can be segregated and reduced at the surface forming, in CO atmosphere, patches of Fe-carbonyl clusters (partly in tight contact with potassium as indicated by the bands at 1794–1762 $cm^{-1}$) and of $K_2C_2O_4$.

The effect of K addition to Fe/$ZrO_2$ is therefore to favor the partial reduction of iron, but this does not lead *per se* to an increased iron dispersion and catalytic activity. The latter, which is promising for butadiene conversion (12, 32, 33), but still to be proved for different reactions such as ethylbenzene dehydrogenation, is probably correlated to the redox equilibrium $Fe^{3+}/Fe^{2+}$ in presence of steam, but not to the further reduction to $Fe^0$. This hypothesis is confirmed by an experiment, here not reported in detail, showing that the adsorption of water (always present in the catalytic reactions discussed above) hinders the formation of the $Fe^0$ carbonyl species by the well known oxidizing action of water on iron.

The experiments reported in the Figs. 3B and 4 show that the desorption and partial decomposition at 523 K of CO adsorbed as Fe-carbonyl produces only partially oxalates, but the new weak bands formed in the range 1600–1300 $cm^{-1}$ can be assigned to carbonate–carboxylate species, formed by a mechanism of CO disproportionation via iron carbonyls. This process refers only to a few carbonyl groups and is not important from the catalytic point of view. A detailed assignment of these groups is not the goal of this paper and is therefore omitted.

The comparison of the FK1 with FK2 and FK3 samples reduced at 773 K, reported in Fig. 6, shows on the samples prepared from iron nitrate at 773 K that a raft-like distribution of iron is obtained, in phases that may or may not contain potassium. The spectra of the adsorbed CO show that part of the catalyst is in the form of the already studied Fe/$ZrO_2$ system (10) (see bands at 2180, 2115–2080 $cm^{-1}$); the other part of the spectrum shows analogies with that of FK1, but the bands at 1794–1762 $cm^{-1}$ are almost completely missing. As their presence is related to the presence of dispersed potassium interacting with iron (2, 6, 19), we can deduce that on these samples potassium is not well mixed with iron and is segregated as separate $K_2CO_3$-like phases. Indeed, previous HREELS results of CO adsorbed on $Fe^0$ monocrystalline faces doped with evaporated potassium (2, 6, 19), and references therein) show several bands, all shifted to lower frequencies (from 1800 to 1750, 1610, down to 1410 $cm^{-1}$ for higher K coverages) with respect to the undoped $Fe^0$ surfaces. The segregated phase can be partially formed of unreduced $K_2CO_3$ (the surface bidentate carbonates give bands at 1650–1600, 1300, and 1050–1020 $cm^{-1}$ (24), visible in Fig. 6, curves b and c) and of potassium, iron(III) trioxalates. The latter compounds are reported in literature (34) to show intense bands at 1710–1650, 1390, and 1270–1250 $cm^{-1}$, all of which present also in our spectra, although the 1390 $cm^{-1}$ band is weaker than expected. The lower intensity of the carbonylic bands is in agreement with the lower iron reducibility in these samples due to the minor interaction with potassium.

The different reducibility of FK2 and FK3 samples can be attributed also to the temperature of calcination (773 instead of 973 K), insufficient to stabilize the mixed Fe–K phases and to reduce the nitrate anion from the precursor; this can also produce a more difficult formation of the mixed $KFeO_2$ dispersed phase. On the FK1 sample the formation of potassium oxalate ex-citrate favors the intermediate KFe(II) oxalates, which, by reduction at increasing temperatures, produce $Fe^0$ clusters, forming, in CO atmosphere, Fe-carbonyls in tight contact with K (see the bands at 1794–1762 $cm^{-1}$) or anionic carbonyl-ferrates stabilized by the $K^+$ counterion. The final result is the higher reducibility, at least on the surface, of the sample containing potassium as FeK-oxalates or $KFeO_2$, with Fe and K in close contact. These phases fully cover the support and hinder the anchoring and stabilization of ferrous ions to the surface of zirconia (10). In Table 2 all the relevant IR bands

formed by CO adsorption are assigned by comparison with the literature data.

The TPR spectra confirm the IR results. The formation and the partial reduction of iron to $Fe^0$ clusters, plus residual amounts of $Fe^{x+}$–CO ($x = 2,3$) species (Fig. 6, curves b and c) is parallelled in the TPR spectra by the incomplete reduction peak ($H_2/Fe < 1.5$) at lower temperature (573–623 K) in both the Fe alone and Fe–K samples prepared ex-iron nitrate (Figs. 9a and 9b). The more complex situation of $Fe^{3+}$ reduction in the ex-citrate samples containing potassium (Fig. 9c) could be explained by assuming the formation of iron–potassium oxalate phases or more likely $KFeO_2$-like phases as is implied by the 2.1 $H_2/Fe$ ratio observed for the large band centered at 765 K which can be accounted for only by assuming a complete reduction of a $KFeO_2$ phase. In agreement with Refs. (5) and (12), the effect of K addition increases to 765 K the temperature of reduction to $Fe^0$, except for a small surface fraction which is reduced at lower temperatures (peaks at 610, 650 K) in agreement with the IR spectra of adsorbed CO. The same peak at 765 K is present also in the TPR spectrum of FK3, albeit with a lower intensity and consistently with the lower K content of this sample. If a 2/1 $H_2/Fe$ reduction stoichiometry is assumed for this peak and if a 1.5/1 $H_2/Fe$ stoichiometry holds for the peak at 623 K, a simple normalization indicates that approximately 20% of the Fe introduced in the FK3 sample remains unreduced. A similar normalization procedure for $Fe/ZrO_2$ (curve a) shows that the fraction of unreduced iron is approximately 40%, so confirming the stabilizing effect of zirconia on Fe(II) (10) and providing evidence for the easier reducibility of iron in catalysts where potassium is present.

The nitric oxide adsorption on FK1 shows results that are similar to those of CO adsorption, as found for the $Fe/ZrO_2$ system (11). The IR spectra of NO adsorbed on supported iron show a broad band with several components in the range 1700–1820 $cm^{-1}$ assigned to mononitrosyl species bound to iron sites with oxidation number between zero and three and with different coordination (21, 35). Besides, nitric oxide dissociates at low coverages on extended metallic iron, leaving a partially oxidized surface exposed to the subsequent NO doses. It is therefore difficult to determine the oxidation state of the iron sites from the spectrum of adsorbed NO, but a good criterion of assignment could be that the frequency blue shifts from less than 1700 $cm^{-1}$ for $Fe^0$ to more than 1820 $cm^{-1}$ for $Fe^{x+}$ ($x = 2,3$) ions as in Ref. (11).

Figure 7 shows a continous blue shift of about 80 wavenumbers, increasing with the coverage and the contact time, of the mononitrosyl band of NO adsorbed at RT on FK1. The reasons for this shift may be numerous and are here summarized: (i) dipole–dipole coupling effects increasing with the NO coverage; (ii) chemical effects induced by electron transfer by adsorbed NO to the surrounding iron sites; (iii) intrinsic surface heterogeneity, as revealed by CO adsorption, due to different metallic clusters or to differently exposed large $Fe^0$ faces; (iv) exposed iron sites, with different oxidation number before the NO adsorption or induced by NO decomposition on the more reduced sites.

However, the initial ~1675 $cm^{-1}$ frequency of adsorbed NO is consistent with a linear nitrosyl species adsorbed on $Fe^0$ sites (11, 21) and the shift to higher frequencies can be attributed to an overlapping of the previously discussed effects: for example a band at 1735 $cm^{-1}$ was found on the $Fe/ZrO_2$ system and was assigned to a NO adsorbed onto $Fe^{(2-x)+}$ reduced sites preexistent or formed by the partial iron oxidation by decomposed NO. However, a comparison of the results of NO adsorbed on $Fe/ZrO_2$ (11) with that of the FK1 sample reduced in the same way evidences that, with the exception of the shoulder at 1803 $cm^{-1}$, the frequencies of NO adsorbed on the sample containing potassium are definitely lowered by ~100 $cm^{-1}$. Also from the point of view of the intensities of adsorbed NO bands, the nitrosyl bands of FK1 are approximately one order of magnitude less intense that those of the sample without potassium. This can be due both to a minor concentration of the surface species for the decrease of the areas (adsorbed NO/Fe mole ratio is 0.04 vs the value of 0.48 for $Fe/ZrO_2$) and/or to a very different band intensity due to the different chemical bonds formed by NO with different sites. This is proved by the differences both in frequency and in resistance to thermal evacuation: on the FK1 (Fig. 7, curve h) the linear nitrosyls are desorbed by thermal evacuation at 423 K, whereas on the $Fe/ZrO_2$ they are resistant up to 623 K because of the strong bond with the oxidized $Fe^{2+}$ or $Fe^{3+}$ sites (11). The weak and broad bands which remain at 1620–1590 $cm^{-1}$ after evacuation are of uncertain assignment. For their position they can be assigned to residual $Fe^0$–NO tilted groups or, more probably, they can be correlated to the broad absorption between 1500 and 1300 $cm^{-1}$ and assigned to nitrate groups formed by NO dissociation (22, 36, 37). The same assignment to nitrate groups can be made for the weak-broad bands at 1506, 1456, and 1410 $cm^{-1}$. However, for these bands theoretical and the experimental shift for the $^{15}NO$ adsorption are coincident (see Fig. 8). Hence, these data could be in better agreement with NO adsorption as nitrosyl groups, strongly red-shifted in stretching frequency because adsorbed on $Fe^0$ sites that are strongly perturbed by neighboring K atoms (analogously to the carbonyl species at 1794–1762 $cm^{-1}$).

Finally, the strong band at 1245 $cm^{-1}$ can be assigned, for its spectral range and intensity, to the $\nu_{3\,asym}$ mode of a nitrito species. In the case of $Fe/ZrO_2$ (11) an analogous assignment to $NO_2^-$ groups chelated to zirconia was made for a band at 1190–1150 $cm^{-1}$. A partner weak band at 1310 $cm^{-1}$ was assigned to the $\nu_1$(sym) mode (22): for FK1 the corresponding band is found at 1327 $cm^{-1}$. From these considerations and from the presence of the same frequencies and

intensities of the IR spectrum of $KNO_2$ and also the weak combination band at 2564 $cm^{-1}$ ($\nu_1 + \nu_3 = 2572$ $cm^{-1}$) (22), it may be inferred that a $KNO_2$ species is formed on the surface, at the same time with the adsorption of NO and with its partial decomposition on the reduced Fe sites. Bonzel (6, 29) hypothesized an equivalent mechanism of adsorbed NO decomposition, with formation of $NO_2$ stabilized as $KNO_2$ on the ionic $K^+$ phase, on $Pt^0$. The thermal resistance of this species up to 600 K is in agreement with findings of the experiment reported in Fig. 7, curve h.

The experiments of labeled NO reported in Fig. 8 fully confirm the overall picture exposed above.

In conclusion, the results of NO adsorption parallel exactly those of CO adsorption, with nitrosyl (carbonyl) complexes formed on reduced iron sites and nitrito (oxalate) species formed on $K^+$. For CO as well as for NO no traces of interaction with the zirconia are found, which implies that it is fully coated by phases containing K and Fe.

## CONCLUSIONS

Previous papers on the Fe/$ZrO_2$ system (10, 11) have shown that iron is highly dispersed, mainly as coordinatively unsaturated $Fe^{2+}$ ion, onto the surface of zirconia after reduction at 623–773 K with CO and NO adsorbed as monocarbonyl or nitrosyl groups on these sites.

The potassium addition to the same system produces a strong decrease of the amounts of adsorbed molecules. The interaction of ferrous ions with the zirconia surface is replaced, in the presence of potassium, by the growth of a potassium ferrite phase containing oxidized iron and potassium in close contact, in agreement with the literature (3–5). This phase fully covers the surface of zirconia and is reduced with $H_2$ at 773 K, producing patches of small $Fe^0$ particles interspersed with K. In CO atmosphere small iron carbonyls partially interacting with potassium and potassium oxalate groups are formed at room temperature according to the scheme

$$KFeO_2 + CO \rightarrow K_2C_2O_4 + Fe_n(CO)_m. \qquad [1]$$

These species decomposed under vacuum at 473–573 K.

By an analogous mechanism NO adsorbs on free iron and potassium sites of the reduced surface, producing mononitrosyl species adsorbed on $Fe^0$ sites (on which NO partially dissociates already to room temperature) and nitrite species on potassium. The higher iron reducibility at the surface of potassium ferrite, at least in absence of water, is attributed to the close contact of iron with potassium in this phase.

## ACKNOWLEDGMENTS

The authors thank the Italian MURST "Progetti di Rilevante Interesse Nazionale" and CNR (both in Rome) for financial support.

## REFERENCES

1. Somorjai, G. A., "Introduction to Surface Chemistry and Catalysis," pp. 477, 498. Wiley–Interscience, New York, 1994.
2. Seip, U., Bassignana, I. C., Küppers, J., and Ertl, G., *Surf. Sci.* **160**, 400 (1985).
3. Muhler, M., Schütze, J., Weseman, M., Rayment, T., Dent, A., Schlögl, R., and Ertl, G., *J. Catal.* **126**, 339 (1990).
4. Muhler, M., Schlögl, R., and Ertl, G., *J. Catal.* **138**, 413 (1992).
5. Stobbe, D. E., van Buren, F. R., van Dillen, A. J., and Geus, J. W., *J. Catal.* **135**, 533 (1992).
6. Bonzel, H. P., *Surf. Sci. Rept.* **8**, 43 (1987).
7. Udovic, T. J., and Dumesic, J. A., *J. Catal.* **89**, 303 (1984).
8. Snell, R., *Appl. Catal.* **37**, 35 (1988).
9. Bartholomew, C. H., *in* "New Trends in CO Activation" (L. Guczi, Ed.). Elsevier, Amsterdam, 1991, and references therein.
10. Guglielminotti, E., *J. Phys. Chem.* **98**, 4884 (1994).
11. Guglielminotti, E., *J. Phys. Chem.* **98**, 9033 (1994).
12. Boot, L. A., Ph.D. thesis, Utrecht (1994); Boot, L. A., van Dillen, A. J., Geus, J. W., van Buren, F. R., and Bongaarts, J. E., *in* Preparation of Catalysts. VI. Studies in Surfactant Science and Catalysis (G. Poncelet, J. Martens, B. Delmon, and P. Grange, Eds.), Vol. 91, p. 159. Elsevier, Amsterdam, 1995; Boot, L. A., van Dillen, A. J., Geus, J. W., and Van Buren, F. R., *J. Catal.* **163**, 186 (1996).
13. Dall'Agnol, C., Gervasini, A., Morazzoni, F., Pinna, F., Strukul, G., and Zanderighi, L., *J. Catal.* **96**, 106 (1985).
14. Rochester, C. H., and Topham, S. A., *JCS Faraday Trans. I* **75**, 1259 (1979).
15. Thiel, P. A., Hrbek, J., Depaola, R. A., and Hoffmann, F. M., *Chem. Phys. Lett.* **108**, 25 (1984), and references therein.
16. Sheppard, N., and Nguyen, T. T., *in* "Advances in Infrared and Raman Spectroscopy," Vol. 5, Chap. 2. Heyden, London, 1978.
17. Seip, U., Tsai, M. C., Christmann, K., Küppers, J., and Ertl, G., *Surf. Sci.* **139**, 29 (1984).
18. Bartosch, C. E., Whitman, L. J., and Ho, W., *J. Chem. Phys.* **85**, 1052 (1986).
19. Paul, J., *Surf. Sci.* **224**, 348 (1989).
20. Guglielminotti, E., *Langmuir* **6**, 1455 (1990).
21. King, D. L., and Peri, J. B., *J. Catal.* **79**, 164 (1983).
22. Laane, J., and Ohlsen, J. R., *Prog. Inorg. Chem.* **27**, 465 (1980).
23. Calderazzo, F., Ercoli, R., and Natta, A., *in* "Organic Synthesis via Metal-Carbonyls" (I. Wender and P. Pino, Eds.), Vol. 1, p. 99. Wiley, New York, 1968.
24. Busca, G., and Lorenzelli, V., *Mater. Chem.* 175 (1981).
25. Miller, F. A., and Wilkens, C. H., *Anal. Chem.* **24**, 1253 (1952).
26. Hoffmann, F. M., Weisel, M. D., and Paul, A. K., *in* "Carbon Dioxide Chemistry: Environmental Issues" (J. Paul and C.-M. Pradier, Eds.). The Royal Society of Chemistry, Cambridge, 1994.
27. Vigouroux, D., Carel, C., and Vallet, P., *CR Acad. Sci. Paris. Sér. C* **265**, 451 (1967).
28. Temperley, A. A., and Pumplin, D. W., *J. Inorg. Nucl. Chem.* **31**, 2711 (1969).
29. Bonzel, H. P., Brodén, G., and Krebs, H. J., *Appl. Surf. Sci.* **16**, 373 (1983).
30. Solymosi, F., and Berkó, A., *Surf. Sci.* **201**, 361 (1988).
31. Hoppe, R., *Angew. Chem.* **20**, 63 (1981).
32. Stobbe, D. E., van Buren, F. R., Hoogenraad, M. S., van Dillen, A. J., and Geus, J. W., *JCS Faraday Trans.* **87**, 1639 (1991).
33. Stobbe, D. E., van Buren, F. R., van Dillen, A. J., and Geus, J. W., *J. Catal.* **135**, 548 (1992).
34. Gouteron, J., *J. Inorg. Nuclear Chem.* **38**, 55 (1976).
35. Kock, A. J. H. M., and Geus, J. W., *Prog. Surf. Sci.* **20**, 165 (1985).
36. Busca, G., and Lorenzelli, V., *J. Catal.* **72**, 303 (1981).
37. Addison, C. C., Logan, N., Wallwork, S. C., and Garner, C. D., *Q. Rev. Chem. Soc.* **25**, 289 (1971).